type laboratory mixer was used to prepare the mix. Cement, fly ash, and sand were first dry mixed for about 2 minutes. Water mixed with superplasticizer and viscosity modifying agent (VMA) was then added gradually and mixed for another 5 to 10 minutes. The cementitious mixture was carefully placed in a pullout specimen mold, where the pullout fibers were preplaced and vibrated slightly using a vibrating table. Specimens casted were covered with plastic sheets and stored at room temperature for 24 hours prior to demolding.

The matrix mix properties are shown in Table 1 and the key properties of the fibers are shown in Table 2.

A servohydraulic testing machine (MTS 810) was used to conduct fiber pullout tests. The applied pullout loading speed was 0.042 in./min (1.07 mm/min), corresponding to a static loading rate of tensile specimens (Kim et al. 2008). The free length of fiber between mortar prism and gripping device was minimized to eliminate the fiber elongation in measuring the fiber slip. A pullout load was measured from the load cell attached between fiber grip system and testing machine cross head; slip history was measured from the linear variable differential transformer (LVDT) installed next to the specimen grip system (Fig. 2).

EXPERIMENTAL RESULTS

Average pullout load versus slip curves for H- and T-fiber embedded in three matrices are shown in Fig. 3(a) and (b). Since both fiber types have different diameters, average pullout stress, induced in the fiber by pullout, versus slip curves are shown in Fig. 3(c) and (d) for comparison. Each curve represents the average of three to five pullout specimens. All specimens for each matrix were prepared from one batch, and the test results were very consistent; for example, the standard deviation of maximum pullout load of T-fiber embedded in mortar with 8.1 ksi (56 MPa) compressive strength is 0.40 lb (1.78 N) where the average maximum pullout load is 35. 03 lb (155.80 N).

Both H-fiber and T-fiber showed slip hardening behavior up to peak load for all three different matrix strengths: M1 (low: 4.1 ksi [28 MPa]), M2 (medium: 8.1 ksi [56 MPa]), and M3 (high: 12.2 ksi [84 MPa]) and maintained fiber pullout mode even in the highest strength matrix (M3) without fiber breakage. The fiber breakage failure mode is most undesirable since it causes brittle failure instead of ductile failure mode at the composite's level.

Average values of key fiber pullout parameters such as pullout stress, pullout energy (or work), equivalent bond strength, and slip capacity are summarized in Table 3(a) and (b). The IMB point was defined by Kim et al. (2008) as the point where the mechanical component of bond became dominant after adhesion and initial friction were fully activated; it stands for Initiation of mechanical bond (IMB) point. This point can also be defined as the maximum contribution due to initial friction and adhesion before the initiation of mechanical bond.

It is observed from Fig. 3 and Table 3 that the pullout behavior of H- and T-fibers is different for the three matrices, M1 (low strength), M2 (medium strength), and M3 (high strength). Pullout load of H-fiber at IMB point is 19.21 lb (85.43 N) for M1, 28.22 lb (125.54 N) for M2, and 30.41 lb (135.26 N) for M3. T- fiber showed stronger influence of matrix strength on the pullout load at IMB point: 6.82 lb (30.34 N) for M1 and 15.38 lb (68.42 N) and 27.43 lb (122.00 N) for M2 and M3, respectively. The effect of matrix strength on pullout stress at IMB point according to the type of fiber (H- and T-fiber) is graphically illustrated in Fig. 4. While the pullout resistance of both fibers increases with an increase in matrix strength, the resistance of H-fiber tapers off at the high matrix strength while that of T-fiber maintains an almost linear increase. However, the maximum pullout stress of T-fiber shows a different trend as the strength of mortar increases. The maximum pullout stress of T-fiber in M3 is lower than that in M2. This difference may be explained by the increase in damage prior to complete pullout with an increase in matrix strength. For T-fiber, the large slip at maximum pullout, which reaches 50% to 70% of embedded length, may damage the tunnel of matrix if the matrix is too brittle. This effect needs to be further ascertained with additional testing.

The pullout energy (or pullout work) also appears to be dependent upon the strength of the matrix. Since the two fibers have different diameter: the diameter of H- fiber is 0.015 in. (0.38 mm); the diameter of T-fiber is 0.012 in. (0.3 mm), the energy based on pullout stress versus slip was calculated to compare the two fibers. (Fig. 5(a)) H-fiber generated 22.5 ksi-in. (3.9 MPa-m) when embedded in M1, 30 ksi-in. (5.3 MPa-m) in M2, and 32.4 ksi-in. (5.7 MPa-m) in M3. Thus, the higher strength matrix yields higher pullout energy. Similarly to the H-fiber, T-fiber showed an increase in pullout energy with an increase in matrix strength; however, the energy values were significantly higher, almost four times, namely, 42.8 ksi-in. (7.5 MPa-m) when embedded in M1, 123.8 ksi-in. (21.7 MPa-m) in M2, and 132.1 ksi-in. (23.1 MPa-m) in M3. Note also that for both fibers, the energy tends to taper off at high strength.

Assuming that the bond strength remains a constant over the entire embedment length, Kim et al. (2007) suggested that an equivalent bond strength, τ_{eq}, could be calculated from the pullout energy obtained from a single fiber pullout test using Eq. (2).

$$\tau_{eq} = \frac{8 \times E_p}{\pi d_f L_f^{\,2}} \qquad [2]$$

where E_p is the area under the pullout load – slip curve, d_f is the diameter or equivalent diameter of fiber, and L_f is the length of fiber with assuming $L_f/2$ as the fiber embedment length. Since the equivalent bond strength is directly proportional to the pullout energy, the equivalent bond strength is also dependent on the strength of matrix. Equivalent bond strength values of T- fiber are 0.72 ksi (5.00 MPa) in M1, 2.10 ksi (14.47 MPa) in M2, and 2.24 ksi (15.44 MPa) in M3, while the equivalent bond strengths of H-fiber are 0.51 ksi (3.51 MPa) in M1, 0.69 ksi (4.74 MPa) in M2, and 0.73 ksi (5.05 MPa) in M3.

These results are graphically compared in Fig. 5(b). Although the pullout energy of T-fiber is much higher (up to four times) than that of H-fiber (Fig. 5(a)) the maximum pullout stress is not very different (Fig. 6(a)). This is because the high pullout energy of T-fiber is due to its high slip capacity before bond decay. Slip capacity is defined as a slip point when the mechanical portion of bond strength loses the most of its capacity. Average slip capacity values according to the type of fiber and matrix are summarized in Table 3(b). The effect of matrix strength on the slip capacity of both fibers is graphically compared in Fig. 6(b). The slip capacities of T-fiber are 0.40 in. (10.19 mm) in M1, 0.45 in. (11.39 mm) in M2, and 0.51 in. (13.02 mm) in M3, whereas the slip capacities of H-fiber are 0.12 in. (2.95 mm) in M1, 0.15 in. (3.69 mm) in M2, and 0.14 in. (3.53 mm) in M3. In summary, the slip capacity of T-fiber is more than three times that of H-fiber in all three different strength matrices.

The higher pullout energy and slip capacity of T-fiber in comparison to H-fiber is due to the different pullout mechanisms of the two fibers. T-fiber will untwist during pullout while the hook in H-fiber straightens up. The pullout of T-fiber generates contacting pressure along the whole embedded length of fiber, thus, generating significant pullout work or energy. For the H-fiber, the work is due primarily to the deformation of the end hook, while the rest of the fiber contributes little. Once the hook straightens up, the pullout load is drops dramatically.

CONCLUSIONS

This study investigated the pullout performance of two deformed high-strength steel fibers, namely, hooked (H-) fiber and twisted (T-) fiber, embedded in cement matrices (M1, M2, and M3) with three different compressive strengths (4.1, 8.1, and 12.2 ksi [28, 56, and 84 MPa]). The tensile strength of the two steel fibers exceeded 304.4 ksi (2100 MPa). The following conclusions can be drawn:

1. Although both H- and T-fibers lead to better performance with an increase in matrix compressive strength, T-fiber showed much more sensitive behavior than H-fiber, that is, T-fiber is more effective in high strength matrices than H-fiber.
2. The pullout load at IMB point for the T-fiber embedded in the highest strength matrix (M3) was three times that for the lowest strength matrix (M1), while the pullout load at IMB point for the H-fiber embedded in M3 was only 58% higher than that in M1.
3. For fibers embedded in the highest strength matrix M3, the equivalent bond strength at the IMB point was respectively 2.02 ksi (13.95 MPa) for T-fiber and 1.30 ksi (8.94 MPa) for H-fiber. At complete pullout, the equivalent bond strength for T-fiber in M3 was 2.24 ksi (15.44 MPa) while that of H-fiber was 0.73 ksi (5.05 MPa). Maintaining a high equivalent bond strength at increasing slip is one key feature and advantage of the T-fiber.
4. The pullout energy (up to complete pullout) and the equivalent bond strength of T-fiber embedded in the highest strength matrix (M3) were more than twice those for the lowest compressive strength matrix (M1), while the pullout energy and equivalent bond strength of H-fiber in M3 was only 44% higher than that in M1.

5. The pullout energy of T-fiber up to complete pullout ranged in value from two to four times that of H-fiber, when the matrix compressive strength increased from 4.1 to 12.2 ksi (28 to 84 MPa).
6. The maximum slip capacity of T-fiber before a sharp decrease in resistance is about three times that of H-fiber and explains the significant difference in pullout energy between the two fibers.

Overall, it can be said that the more effective performance of T-fiber, compared to the H-fiber, when embedded in a high strength cementitious matrix is based on its unique pullout mechanism during pullout. While both fibers utilize their mechanical bond during pullout, the untwisting behavior of T-fiber provides significantly higher slip prior to pullout stress deterioration, leading to a superior performance overall. Thus, T-fibers should be particularly suitable for high-strength cementitious matrices.

ACKNOWLEDGMENTS

The research described here was sponsored in part by the National Science Foundation (under Grants CMS 0408623 and 0754505), and by the University of Michigan. Their support is gratefully acknowledged. The opinions expressed in this paper are those of the authors and do not necessarily reflect the views of the sponsor.

REFERENCES

Naaman, A.E., and Najm, H., “Bond-Slip Mechanisms of Steel Fibers in Concrete,” *ACI Materials Journal*, V. 88, No. 2, Apr. 1991, pp. 135-145.

Naaman, A.E., and Reinhardt, H.W., 1996, “Characterization of High-Performance Fiber-Reinforced Cement Composites,” *High-Performance Fiber-Reinforced Cement Composites: HPFRCC 2*, Chapter 41, Proceedings of 2nd International Workshop on HPFRCC, A.E. Naaman and H.W. Reinhardt, eds., RILEM, No. 31, E&FN Spon, London, UK, pp. 1-24.

Graybeal, B.A., “Compressive Behavior of Ultra-High-Performance Fiber-Reinforced Concrete,” *ACI Materials Journal*, V. 104, No. 2, Mar.-Apr. 2007, pp. 146-152.

Kim, D.J.; El-Tawil, S.; and Naaman, A.E., “Loading Rate Effect on Pullout Behavior of Deformed Fiber,”*ACI Materials Journal*, V. 105, No. 6, Nov.-Dec. 2008, pp. 576-584.

Kim, D.J.; El-Tawil, S.; and Naaman, A.E., “Correlation between Single Fiber Pullout Behavior and Tensile Response of FRC Composites with High-Strength Steel Fiber,” *Proceedings of RILEM International Workshop on High-Performance Fiber-Reinforced Cement Composites—HPFRCC5*, Germany, H.W. Reinhardt and A.E. Naaman, eds., Pro. 53, S.A.R.L., Cachan, France, July 2007, pp. 67-76.

Kim, D.J.; El-Tawil, S.; and Naaman, A. E., “Rate-Dependent Tensile Behavior of High-Performance Fiber-Reinforced Cementitious Composites,” *Materials and Structures*, V. 42, No. 3, 2009, pp. 399-414.

Habel, K.; Viviani, M.; Denarie, E., and Brühwiller, E., “Development of the Mechanical Properties of an Ultra-High-Performance Fiber-Reinforced Concrete (UHPFRC),” *Cement and Concrete Research*, V. 36, No. 7, July 2006, pp. 1362-1370.

Shannag, M.J.; Brincker, R.; and Hansen, W., “Interfacial (Fiber-Matrix) Properties of High-Strength Mortar (150 MPa) from Fiber Pullout,” *ACI Materials Journal*, V. 93, No. 5, Sept.-Oct. 1996, pp. 1-7.

Robins, P.; Austin, S.; and Jones, P., “Pull-Out Behavior of Hooked Steel Fibers,” *Materials and Structures*, V. 35, Aug. 2002, pp. 434-442.

Rossi, P., “Development of New Cement Composite Materials for Construction,” Proceedings of the Institution of Mech. Engineers, Part L, *Journal of Materials: Design and Applications*, V. 219, No. 1, 2005, pp. 67-74.

Chan, Y.-W., and Chu, S.-H., “Effect of Silica Fume on Steel Fiber Bond Characteristics in Reactive Powder Concrete,” *Cement and Concrete Research*, V. 34, 2004, pp. 1167-1172.

Table 1—Composition of matrix mixtures by weight ratio and compressive strength

Matrix	Cement (Type III)	Fly ash*	Sand† (flint)	Silica fume	Super - plasticizer	VMA‡	Water	f_c', ksi (MPa)
M1	0.70	0.30	3.50	—	0.009	0.024	0.65	4.1 (28)
M2	1.00	0.15	1.00	—	0.009	0.006	0.35	8.1 (56)
M3	0.80	0.20	1.00	0.07	0.04	0.012	0.26	12.2 (84)

*Type C.

†ASTM 50-70.

‡Viscosity modifying agent.

Table 2—Properties of high-strength hooked and twisted fibers

Fiber type	Diameter, in. (mm)	Length, in. (mm)	Density g/cc	Tensile strength, ksi (MPa)	Elastic modulus, ksi (GPa)
Hooked	0.015 (0.38)	1.18 (30)	7.9	304 (2100)	29,000 (200)
Twisted	0.012 (0.3)*	1.18 (30)	7.9	400 (2760)†	29,000 (200)

*Equivalent diameter.

†Tensile strength of fiber after twisting.

Table 3—Single fiber pullout test results

(a) IMB point

Matrix composition			M1	M2	M3
Pullout energy	H-fiber	lb-in.	1.08	1.47	1.43
		N-mm	123	167	161
	T-fiber	lb-in.	0.92	1.67	3.18
		N-mm	104	189	360
Pullout stress energy	H-fiber	ksi-in.	5.6	7.6	7.3
		MPa-m	1.0	1.3	1.3
	T-fiber	ksi-in.	8.4	15.3	29.1
		MPa-m	1.5	2.7	5.1
Equivalent bond strength	H-fiber	ksi	0.92	1.25	1.21
		MPa	6.34	8.61	8.34
	T-fiber	ksi	0.59	1.06	2.02
		MPa	4.05	7.33	13.95
IMB pullout load	H-fiber	lb	19.21	28.22	30.41
		N	85.43	125.54	135.26
	T-fiber	lb	6.82	15.38	27.43
		N	30.34	68.42	122.00

(b) Complete pullout

Matrix composition			M1	M2	M3
Pullout energy	H-fiber	lb-in.	4.39	5.92	6.32
		N-mm	496	669	714
	T-fiber	lb-in.	4.68	13.57	14.48
		N-mm	529	1533	1636
Pullout stress energy	H-fiber	ksi-in.	22.5	30.4	32.4
		MPa-m	3.9	5.3	5.7
	T-fiber	ksi-in.	42.8	123.8	132.1
		MPa-m	7.5	21.7	23.1
Equivalent bond strength	H-fiber	ksi	0.51	0.69	0.73
		MPa	3.51	4.74	5.05
	T-fiber	ksi	0.72	2.10	2.24
		MPa	5.00	14.47	15.44
Maximum pullout load	H-fiber	lb	28.71	36.15	42.72
		N	127.71	160.80	190.05
	T-fiber	lb	13.69	35.03	31.30
		N	60.88	155.80	139.21
Slip capacity	H-fiber	in.	0.12	0.15	0.14
		mm	2.95	3.69	3.53
	T-fiber	in.	0.40	0.45	0.51
		mm	10.19	11.39	13.02

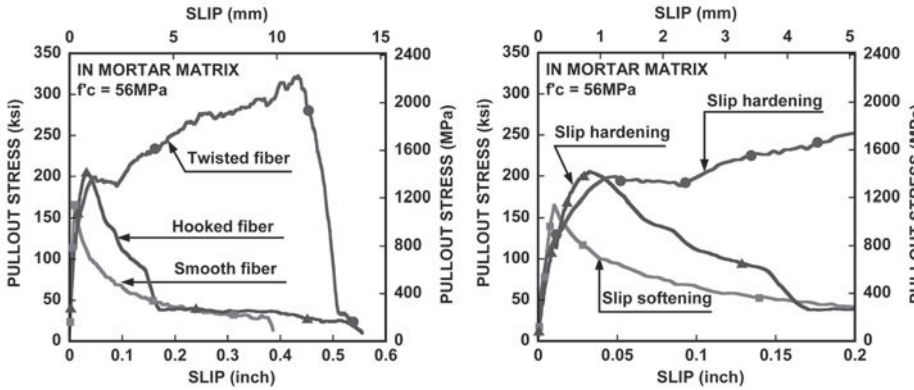

Fig. 1—Slip hardening (T- and H-fiber) and softening (smooth fiber) pullout behavior: (a) full-slip scale; and (b) magnified scale to show initial portions of curves.

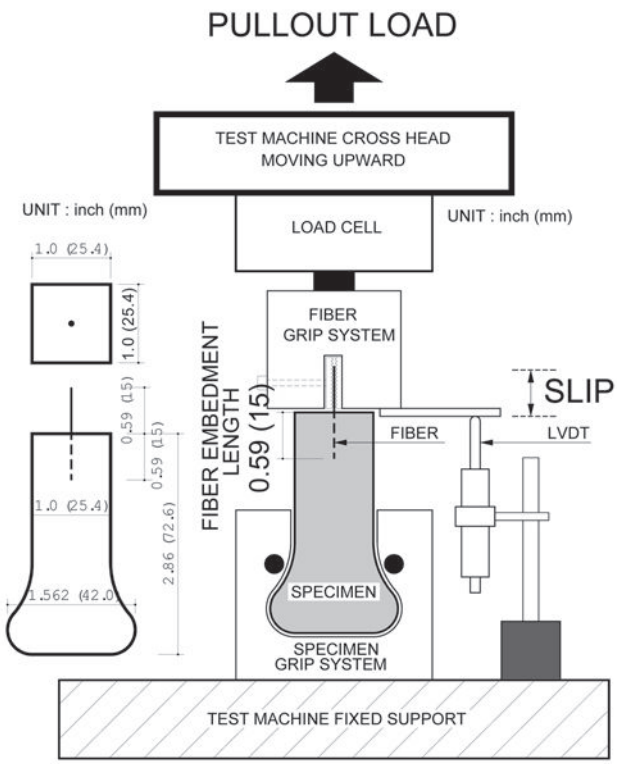

Fig. 2—Pullout test specimen and setup.

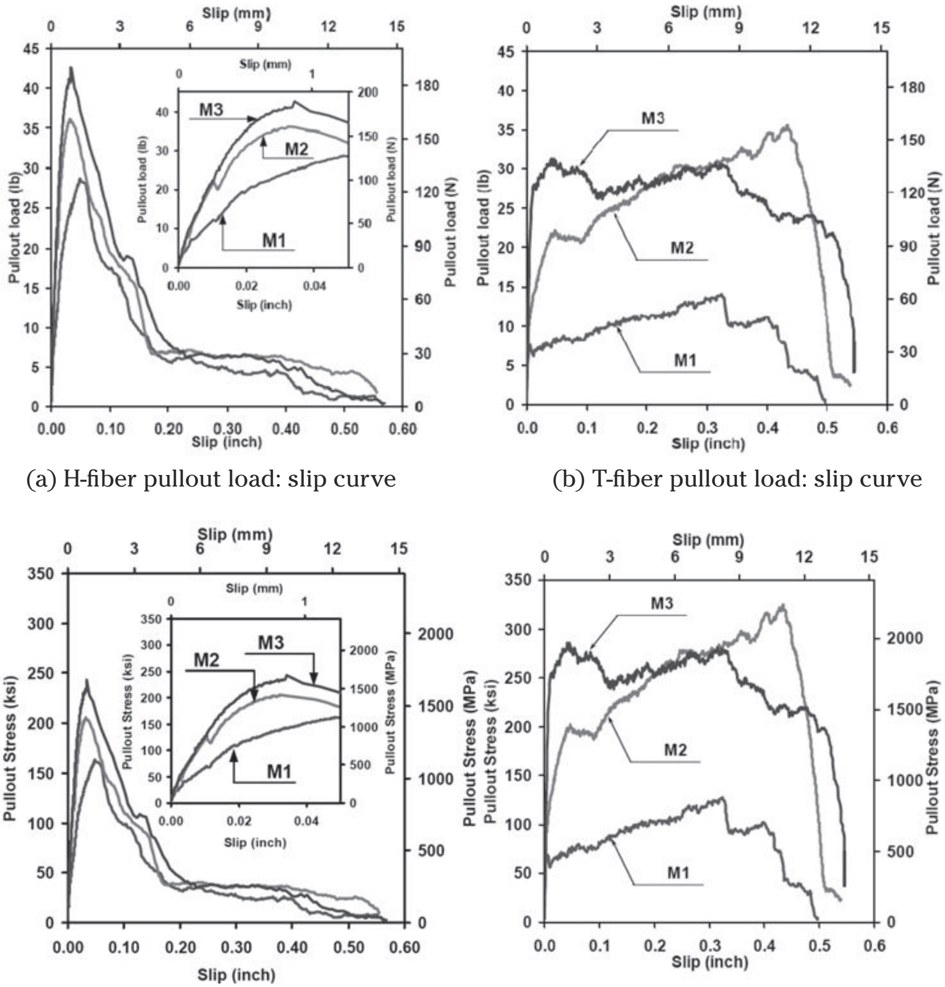

(a) H-fiber pullout load: slip curve

(b) T-fiber pullout load: slip curve

(c) H-fiber pullout stress: slip curve

(d) T-fiber pullout stress: slip curve

Fig. 3—Single fiber pullout test results: average curve.

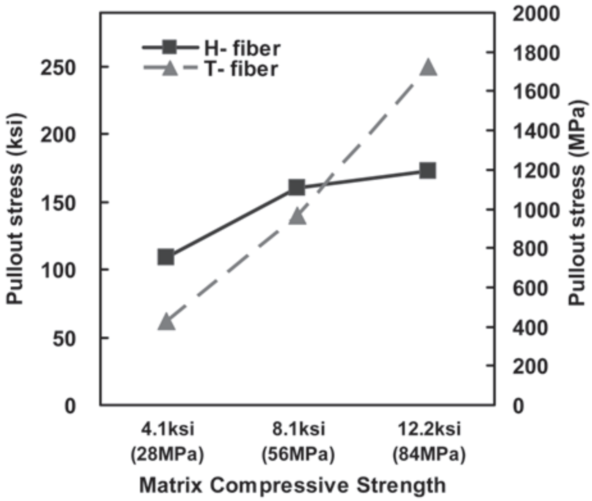

Fig. 4—Effect of matrix strength on pullout stress at IMB point.

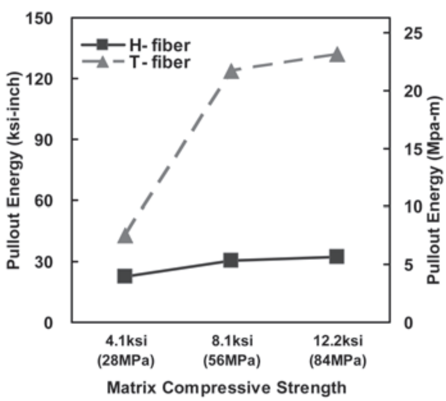

(a) Pullout stress energy

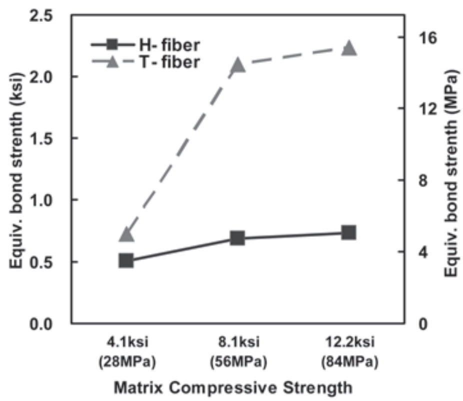

(b) Equivalent bond strength

Fig. 5—Effect of matrix strength on complete pullout energy and equivalent bond strength.